HOKKAIDO UNIVERSITY

Title	Mechanical and thermal stimuli-induced release of toluene included in luminescent crystals as one-dimensional solvent channels
Author(s)	Sagara, Yoshimitsu; Takahashi, Kiyonori; Nakamura, Takayoshi; Tamaoki, Nobuyuki
Citation	Journal of materials chemistry C, 8(29), 10039-10046 https://doi.org/10.1039/d0tc02473b
Issue Date	2020-08-07
Doc URL	http://hdl.handle.net/2115/82429
Type	article (author version)
File Information	Sagara_MCL_crystal__toluene_channels_revised.pdf

Instructions for use

Hokkaido University Collection of Scholarly and Academic Papers : HUSCAP

ARTICLE

Mechanical and Thermal Stimuli-induced Release of Toluene Included in Luminescent Crystals as One-dimensional Solvent Channels

Received 00th January 20xx,
Accepted 00th January 20xx

DOI: 10.1039/x0xx00000x

Yoshimitsu Sagara,*[a,b] Kiyonori Takahashi,[c] Takayoshi Nakamura,[c] Nobuyuki Tamaoki[c]

Luminescent materials that change their photophysical properties and molecular arrangement in response to external stimuli have attracted attention because of the potential application in sensors, memories, security inks, and informational displays. The combination of external stimuli-responsive luminescence with the release of volatile molecules would give more sophisticated photofunctional materials. Herein we discuss a 9,10-bis(phenylethynyl)anthracene derivative that formed green-emissive crystals containing one-dimensional toluene channels. Amide groups of the compounds formed linear hydrogen-bonds in the crystals. Thermal treatment resulted in a phase transition to another crystalline state with the release of the guest toluene molecules. However, little alteration in the photoluminescent properties occurred during the transition. Mechanical stimuli led to the release of volatile molecules along with an emission colour change with a transition from the crystalline to an amorphous phase. Infrared spectroscopy showed that linear hydrogen bonds remained after a thermal treatment-induced phase transition, whereas mechanical stimuli disturbed them.

Introduction

Luminescent organic/organometallic materials that change their photophysical properties in response to thermal treatment and/or mechanical stimuli have been explored to understand their fundamental mechanism and potential applications.[1-27] Normally, external stimuli-induced alteration in the arrangement of luminophores leads to thermoresponsive or mechanoresponsive luminescence. Combining such properties with other dynamic molecular functions, such as the release of small molecules[28,29] and photo-induced dimerisation[30] gives more sophisticated photofunctional materials. Despite an increasing number of mechanochromic luminescent compounds,[30-65] only a few of them can exhibit the release of small molecules concomitant with emission colour change when mechanically stimulated.[28,29]

The effective release of small molecules requires appropriate molecular arrangements.[66,67] Introducing functional groups into the molecular stuctures, that can form hydrogen bonds, can align fluorophores in crystals, supramolecular fibers, and liquid crystals.[4,68-85] Therefore, hydrogen bonds can be utilised to produce stimuli-responsive luminescent molecular structures containing channels filled with small molecules that can be released. Furthermore, the competing effects of hydrogen bonding and π-π stacking result in several thermodynamically (meta)stable states that can be converted from one form to another by thermal treatment, mechanical stimuli, and exposure to solvent vapour.[31,35,38,39,47,54,65,86,87] This is because the length between functional groups forming hydrogen bonds is generally longer than the distance between aromatic moieties constructing π-π stacked structures.[31,35,38,65] Since it was discovered that a 1,3,6,8-tetraphenylpyrene derivative having four hexylamide groups was found to show mechanochromic luminescence,[31] several organic compounds have been reported to form hydrogen bonds in their molecular assemblies and change their emission colours in response to mechanical and thermal stimuli.[35,38,39,47,86-88] Most recently, our group reported on mechanochromic luminescence exhibited by a 9,10-bis(phenylethynyl)anthracene derivative with two amide groups by which it forms two-dimensional, hydrogen-bonded molecular sheets in crystals.[65] However, no crystals containing other small guest molecules were produced from the various solvent mixtures tried for recrystallisation. Here, we demonstrated that another 9,10-bis(phenylethynyl)anthracene derivative formed one-dimensionally hydrogen-bonded columnar assemblies in crystals, and channels of small molecules surrounded by one-dimensional luminophore columns. After thermal or mechanical stimulus, the guest molecules were released from the crystals. In the latter case, a

[a] Department of Materials Science and Engineering, Tokyo Institute of Technology, 2-12-1, Ookayama, Meguro-ku, Tokyo 152-8552, Japan.
E-mail: sagara.y.aa@m.titech.ac.jp
[b] JST-PRESTO, Honcho 4-1-8, Kawaguchi, Saitama 332-0012, Japan.
[c] Research Institute for Electronic Science, Hokkaido University, N20, W10, Kita-ku, Sapporo, Hokkaido 001-0020, Japan.

†Electronic Supplementary Information (ESI) available: Synthesis of compound **1**, crystallographic data, additional PXRD, DSC, NMR measurements, and additional Figures on the photophysical properties. See DOI: 10.1039/x0xx00000x

Please do not adjust margins

clear change of emission colour from green to yellow occured at the same time.

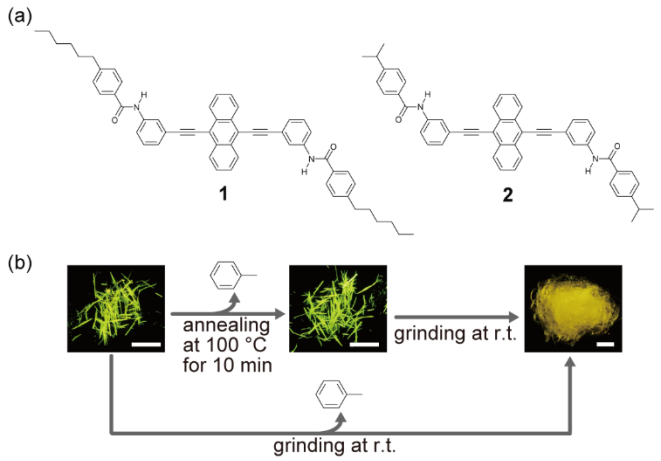

Fig. 1 (a) Molecular structures of two 9,10-bis(phenylethynyl)anthracene derivatives **1** and **2**. (b) Thermal and mechanical stimuli-responsive luminescent behaviour of crystals composed of compound **1** and toluene as the guest molecules. Scale bar: 3 mm. The emission images were taken under excitation at 365 nm.

Results and discussion

A new 9,10-bis(phenylethynyl)anthracene derivative **1** was designed to have two amide groups (Fig. 1a). These amide groups were used to introduce the hexylphenyl groups to the luminophore instead of the isopropyl groups used in compound **2**, which has been reported to form two-dimensionally hydrogen-bonded molecular sheets in crystals.[65] The use of hexylphenyl groups was expected to enhance the solubility of the compound and also prevent the two-dimensional hydrogen-bonding formation, which would have insufficient space to include the guest molecules.

Compound **1** was synthesized via a Sonogashira coupling reaction between 9,10-dibromoanthracene and *N*-(3-ethynylphenyl)-4-hexylbenzamide. The new 9,10-bis(phenylethynyl)anthracene derivative **1** showed enhanced solubility in some common organic solvents compared to compound **2**. This was because of the moderately flexible 4-hexylphenyl substituents, which allowed for easy purification of the compound (see supporting information). Compound **2** only dissolved well in hot DMF and DMSO,[65] whereas compound **1** was soluble in THF, chloroform, DMF, and DMSO at room temperature (r.t.).

Compound **1** crystals were produced when recrystallized from a mixture of toluene and DMF (30/1, v/v). Fig. 1b depicts the thermal and mechanical stimuli-induced phase transition behaviour of the crystals. On heating, the green emissive crystals (**1Cr•Tol**) (Fig. 1b, left), which contained toluene molecules as the solvent channels (see below), transitioned to a different crystalline state (**1Cr**) accompanied with the release of the guest toluene. The green photoluminescence under excitation light of 365 nm was retained during the phase transition. When **1Cr** was ground at r.t., it transitioned to an amorphous state (**1Am**) occurred, and the photoluminescence

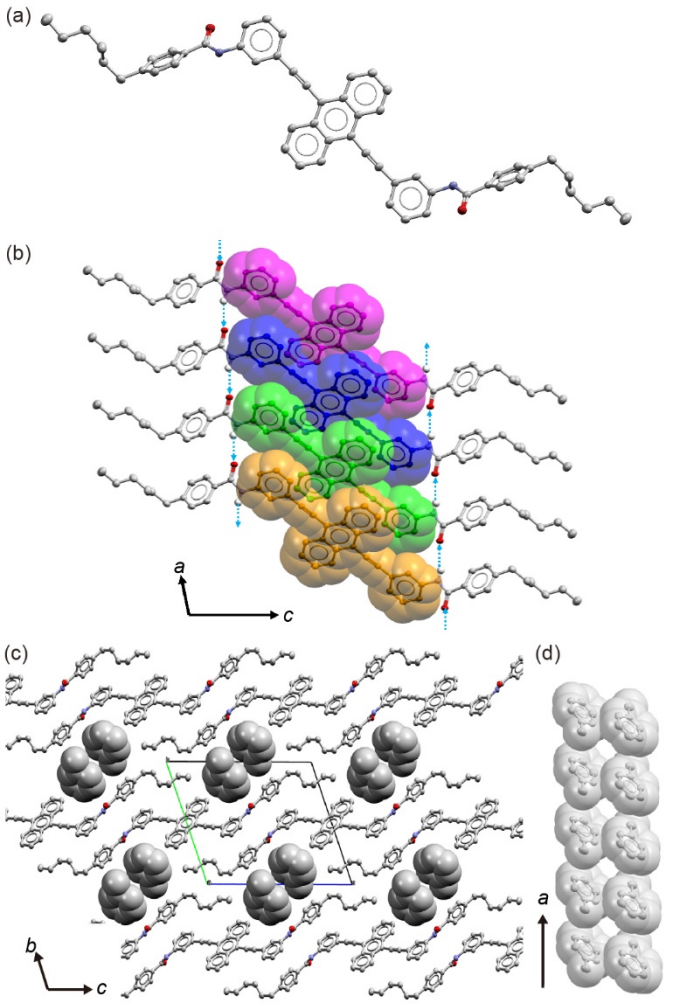

Fig. 2 Crystal structure of **1Cr•Tol**. Carbon, hydrogen in (b), oxygen, and nitrogen atoms are coloured as grey, white, red, and blue, respectively. (a) Molecular structure of compound **1** in the crystal **1Cr•Tol**. (b) The π-π stack assembly of **1** in **1Cr•Tol** viewed along the *b* axis. The 9,10-bis(phenylethynyl)anthracene structure is represented by the space filling model with different colours, and other atoms are depicted by thermal ellipsoid model with 50% probability. (c) Packing structure of crystal **1Cr•Tol** viewed along the *a* axis. Toluene molecules are shown as space filling, and compound **1** is shown as a thermal ellipsoid model. (d) An array of toluene molecules included in a one-dimensional void along the *a* axis. All hydrogen atoms are omitted except those involved in hydrogen bonds in (b).

colour changed from green to yellow. Direct conversion from **1Cr•Tol** to **1Am** was also achieved by mechanical grinding at r.t., which meant both the release of the guest toluene and emission colour change occurred concomitantly.

Single crystal X-ray structure analysis clarified the molecular assembled structures in **1Cr•Tol** (Fig. 2). The **1Cr•Tol** crystal is comprised of two toluene per one compound **1**. Fig. 2a shows the molecular structure of compound **1** in the crystal. The atoms of the 9,10-bis(phenylethynyl)anthracene structure were located almost in the plane, whereas the phenylene rings in the terminal 4-hexylphenyl groups were tilted 73.04° to the luminophore plane. Fig. S1 shows the crystallographically independent molecular structure of compound **1** in **1Cr•Tol**. The compound **1** half structure and one toluene molecule were crystallographically independent, and the symmetrical

This journal is © The Royal Society of Chemistry 20xx

Please do not adjust margins

inversion center coincided with the central position of the anthracene ring in compound **1**. As shown in Table S1, the crystal system and space group of **1Cr•Tol** were triclinic and $P\bar{1}$, respectively.

Fig. 2b shows the π-π stack assembly of compound **1** in **1Cr•Tol**. The compound **1** luminophores were stacked in parallel along the *a* axis. The distances between the adjacent luminophores planes and between centres of adjacent luminophores were 3.240 and 5.290 Å, respectively. Therefore, the luminophores were assembled by offset face-to-face π-π interaction along the *a* axis. The amide groups of the compound **1** formed linear hydrogen bonds along the *a* axis, forming a one-dimensional (1D) column by competing with the π-π stack. The strength of the hydrogen bond was moderate,[89] because the distance between the N•••O atoms and N-H•••O angle were 3.164 Å and 158.96°, respectively.

Fig. 2c shows the packing structure of **1Cr•Tol** when viewed along the *a* axis. The compound **1** 1D columns did not interact with the adjacent 1D columns in the *b* axis within the van der Waals radius, but they hydrophobically interacted, where alkyl chains interdigitated. In addition, the carbonyl C atom interacted with the H atom at the luminophore edge within the van der Waals radius between the 1D columns adjacent in the *c* axis. The corresponding distance between C•••H atoms and angles of C-H•••C atoms were 2.879 Å and 134.53°, respectively (Fig. S2). Considering that compound **2** formed a two-dimensionally hydrogen-bonded molecular sheet,[65] the hexyl groups introduced to compound **1** plays a pivotal role in forming 1D columnar structures.

1Cr•Tol crystals had 1D voids along the *a* axis, in which crystallized toluene were included (Fig. 2c, d). The toluene methyl group was oriented anti-parallel to cancel the dipole moment with the adjacent toluene molecule in the [011] direction (Fig. 2d). The toluene π planes were stacked in parallel along the *a* axis. The closest interatomic distance between the adjacent toluene π plane C atoms and the distance between the toluene π plane centroid were 3.728 Å and 5.290 Å, respectively. Therefore, toluene was stacked with weak π•••π interactions.[90] These analyses indicated that the crystallized toluene molecules in the 1D channel were stabilized by dipole-dipole and weak π•••π interactions.

Next, we examined the thermal stimuli-induced release of toluene during the transition from **1Cr•Tol** to **1Cr**. A differential scanning calorimetry (DSC) trace recorded for **1Cr•Tol** on heating displayed two endothermic peaks at 67.5 and 247.8 °C (Fig. 3a). The former peak was ascribed to the transition from **1Cr•Tol** to **1Cr**, whereas the latter corresponded to the transition to the isotropic state. The trace became non-flat after melting because of the gradual decomposition of the compound, which was confirmed by polarized optical microscopy (Fig. S3). Thermogravimetric analysis (TGA) conducted for **1Cr•Tol** suggested the release of toluene from 1D channels during the transition from **1Cr•Tol** to **1Cr**. As shown in Fig. 3b, the sample weight decreased at around 70 °C. Approximately 18% of the initial weight was reduced, which coincided with the total amount of toluene included in **1Cr•Tol**. The release of toluene

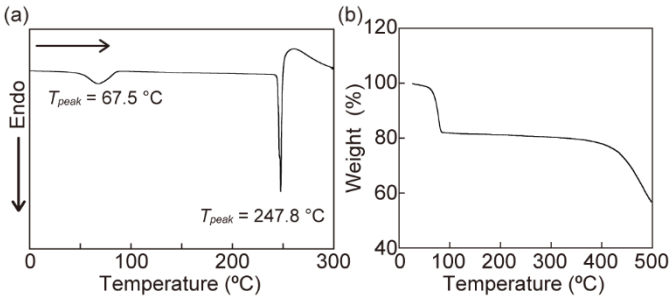

Fig. 3 (a) A DSC trace and (b) a TGA trace recorded for **1Cr•Tol** on heating. Both measurements were performed under nitrogen. The scanning rate was 10 °C min^{-1}.

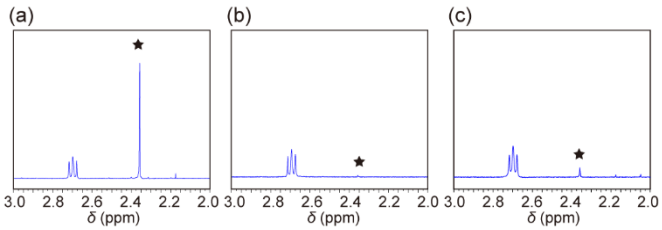

Fig. 4 Partial ^{1}H NMR spectra of (a) **1Cr•Tol**, (b) **1Cr**, and (c) **1Am** in $CDCl_3$. The "star" symbols indicate singlet peaks ascribed to the methyl group of toluene. All measurements were performed at r.t.

was confirmed by ^{1}H NMR measurements (Fig. 4a, b). A singlet peak ascribed to the toluene methyl group was observed at 2.36 ppm when the **1Cr•Tol** crystal dissolved in a $CDCl_3$ solution. The methylene protons next to the phenyl group of compound **1** gave a triplet peak around 2.7 ppm. In contrast, the singlet peak almost disappeared when measured from a crystalline sample that was annealed at 100 °C for 10 min (Fig. 4b), though the partial ^{1}H NMR chart displayed the triplet peak corresponding to **1**.

The change in molecular assembled structures on transition from **1Cr•Tol** to **1Cr** was clarified by PXRD patterns. Crystalline **1Cr•Tol** displayed many sharp peaks in the diffractogram (Fig. 5a). After thermal treatment, some broad peaks were observed at different positions from those of **1Cr•Tol** (Fig. 5b). The peak broadening meant **1Cr** no longer had well-ordered molecular assembled structures, which coincided with the fact that the crystal structure was not solved on the single crystal X-ray structure analysis after thermal treatment.

Infrared spectroscopic measurements were performed to clarify whether the transition affected the hydrogen bonding mode in the condensed state (Fig. 6). The initial crystal **1Cr•Tol** showed sharp bands corresponding to N-H and C=O stretching at 3335 and 1649 cm^{-1}, respectively. The band positions indicated that the amide groups of **1** formed hydrogen bonds in the crystal, as revealed by single crystal structural analysis (Fig. 2). Both peaks showed shifts to a higher wavenumber region after thermal treatment (Fig. 6a → Fig. 6b). This comparison revealed that thermal treatment led to not hydrogen bond breakage but slight changes in the hydrogen bonding mode. This was caused by the alteration in the molecular arrangement and release of toluene on phase transition from **1Cr•Tol** to **1Cr**.

We also investigated the mechanical stimuli-induced release of toluene from **1Cr•Tol**. As shown in Fig. 5c, no peaks

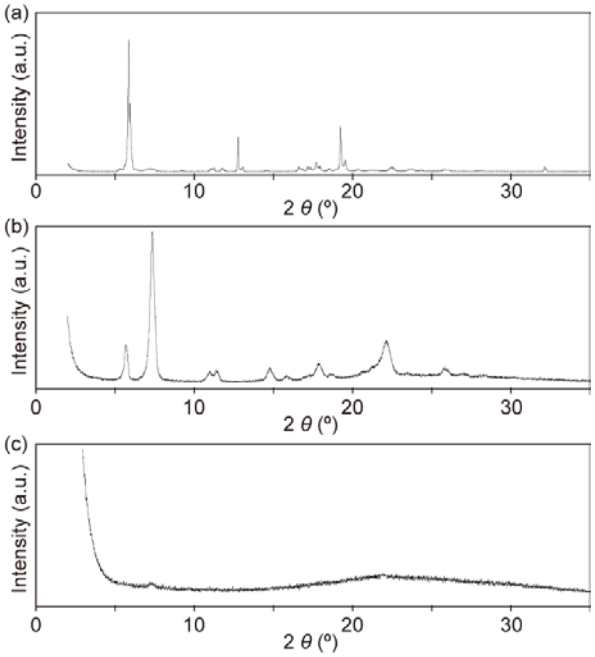

Fig. 5 PXRD patterns recorded for (a) **1Cr•Tol**, (b) **1Cr**, and (c) **1Am**. All measurements were performed at r.t.

were observed in the PXRD pattern after mechanical grinding to **1Cr•Tol** at r.t. The unambiguous change clarified that the molecular assembled state became amorphous. The ground sample (**1Am**) displayed an exothermic peak at 100.7 °C on the heating trace during the DSC measurement (Fig. S4) instead of the endothermic peak observed for the initial **1Cr•Tol** crystalline sample. As the peak was exothermic, **1Am** is thermodynamically metastable. It is noteworthy that **1Am** was converted to the other solid phase after the thermal treatment because the emission intensity significantly decreased. Regarding the infrared spectra (Fig. 6), the two bands ascribed to N-H and C=O stretching became very broad compared to the bands observed for the two crystalline phases. These results indicated that mechanical grinding disturbed the linear

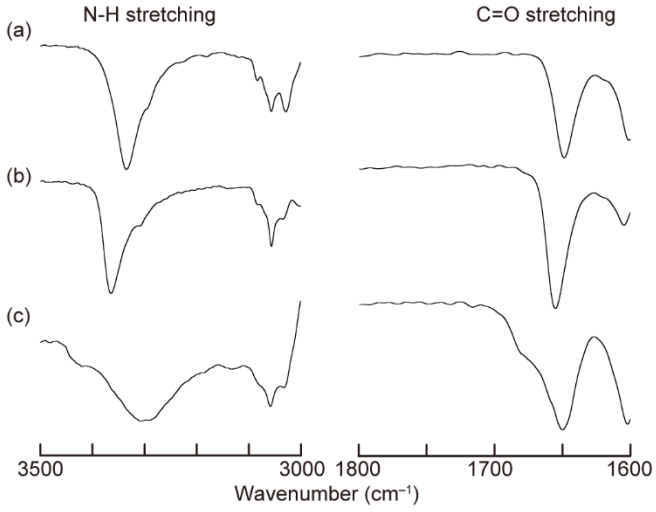

Fig. 6 Partial IR spectra of (a) **1Cr•Tol**, (b) **1Cr**, and (c) **1Am**. All spectra were measured at r.t.

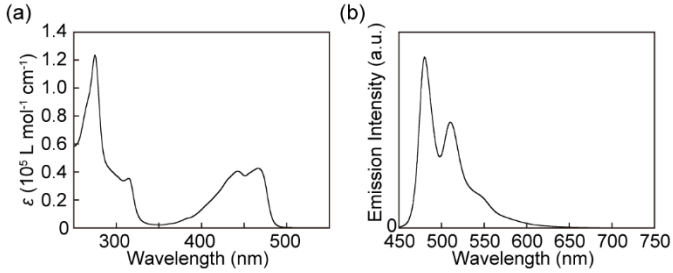

Fig. 7 (a) Absorption and (b) fluorescence spectra of compound **1** in chloroform (c = 1.0 $\times 10^{-5}$ M). The excitation wavelength for the fluorescence spectrum was 400 nm. Both spectra were recorded at r.t.

hydrogen bonding mode without any cleavage of the hydrogen bonds. Similar mechanical stimuli-induced changes in IR spectra have been reported for several mechanochromic luminescent materials.[31,38,65] The mechanical stimuli-induced release of toluene was clarified by ^{1}H NMR measurements. A $CDCl_3$ solution that dissolves **1Am** immediately after grinding gave a faint peak at 2.36 ppm on the ^{1}H NMR chart (Fig. 4c). It took two weeks to remove the included toluene from **1Cr•Tol** under vacuum at r.t. until the remaining toluene amount became almost the same as that in **1Am** (Fig. S5). Therefore, we concluded that toluene molecules were released upon mechanical grinding. Since, the 1D channel structures in **1Cr•Tol** were broken upon grinding, a small amount of toluene was trapped in **1Am**, giving a small singlet peak at 2.36 ppm.

The photophysical properties of **1Cr•Tol**, **1Cr**, and **1Am** were investigated to clarify the mechanism of the thermal and mechanical stimuli-responsive behaviour. Absorption and fluorescent spectra of the chloroform solution of **1** (c = 1.0 $\times 10^{-5}$ M) are shown in Fig. 7. The solution gave an absorption band between 400 and 500 nm (Fig. 7a). Two peaks appeared at 467 and 442 nm with molar extinction coefficients of 4.2 $\times$ 10^4 L mol^{-1} cm^{-1} and 4.0 $\times$ 10^4 L mol^{-1} cm^{-1}, respectively. Another absorption peak was also observed at 275 nm with a relatively large molar extinction coefficient of 1.2 $\times$ 10^5 L mol^{-1} cm^{-1}. In the fluorescence spectrum, well-resolved vibronic structures were observed, suggesting that compound **1** was well-individualised in chloroform (Fig. 7b). The emission spectrum displayed two peaks and one shoulder at 480, 510, and 548 nm, respectively. Several 9,10-bis(phenylethynyl)anthracene derivatives have also been reported to show similar spectral features.[18,39,53,91-93]

Photoluminescence spectra of **1Cr•Tol**, **1Cr**, and **1Am** were compiled in Fig. 8. Crystalline **1Cr•Tol** displayed an emission

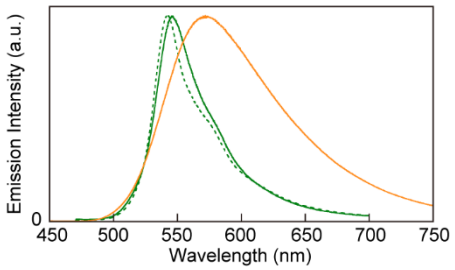

Fig. 8 Photoluminescence spectra of **1Cr•Tol** (green solid line), **1Cr** (green dotted line), and **1Am** (orange solid line) at r.t. The excitation wavelength for all spectra was 400 nm.

This journal is © The Royal Society of Chemistry 20xx

Please do not adjust margins

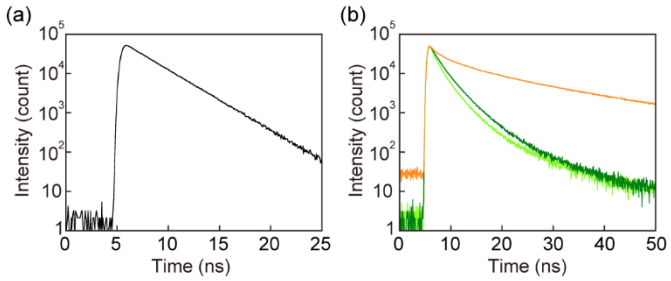

Fig. 9 (a) An emission decay profile of the chloroform solution of compound **1**. (b) Emission decay profiles recorded for **1Cr•Tol** (green line), **1Cr** (light green line), and **1Am** (orange line) at r.t. All decay profiles were monitored with excitation at 405 nm.

peak and a shoulder at 545 and 580 nm, respectively. After the thermal stimuli-induced release of toluene, **1Cr** displayed the emission spectrum at almost the same wavelength region as **1Cr•Tol**, though the emission peak showed a slight blueshift (545 → 542 nm). In contrast to the thermal stimuli-induced transition from **1Cr•Tol** to **1Cr**, the mechanical stimuli-induced release of toluene was accompanied with a significant change in the photoluminescence properties as shown in Fig. 1b. The emission spectral feature of amorphous **1Am** were different from those of the crystalline states, **1Cr•Tol** and **1Cr**. The broad and structureless emission band, which is a typical spectral feature of excimers, peaked at 573 nm. Photoluminescence quantum yields of **1Cr•Tol**, **1Cr**, and **1Am** were 0.18, 0.17, and 0.34, respectively.

Emission lifetime measurements were conducted to understand the stimuli-responsive photoluminescence properties. A chloroform solution of **1** showed a simple emission decay, reflecting their isolated character in the solution (Fig. 9a). The profile fitted well with a single exponential decay function, and the calculated lifetime was 2.8 ns, which is an emission lifetime of the monomer. Crystalline states of **1Cr•Tol** and **1Cr** gave similar decay profiles that could be fitted with a triexponential decay function (Fig. 9b). The resultant lifetimes obtained from **1Cr•Tol** were 1.4, 3.1, and 9.1 ns, while **1Cr** gave emission lifetimes of 1.2, 2.8, and 9.0 ns. Yellow-emissive amorphous state **1Am** displayed a profile that could be fitted with a multi-exponential decay function (Fig. 9b, orange line), and a relatively long emission lifetime of 21 ns was obtained. The longer emission lifetime supported the excimer formation between the luminophores in **1Am** as described above.

It is noteworthy that the amorphous **1Am** was also obtained by grinding **1Cr** at r.t. as shown in Fig. 1b, though no release of toluene occurred in this case. Ground **1Cr** showed no clear peaks in the PXRD pattern (Fig. S6), which clarified the amorphous nature of the ground state. Furthermore, the emission spectrum became broad and structureless (Fig. S7a), and a similar emission decay profile to that of **1Am** was obtained (Fig. S7b). All data mentioned here indicated that ground **1Cr** is amorphous **1Am**.

The change in emission colour from green to yellow (Fig. 1b) was caused by mechanical stimuli-induced excimer formation between the luminophores. In **1Cr•Tol** and **1Cr**, the linear hydrogen bonds between amide groups arranged the 9,10-bis(phenylethynyl)anthracene groups with offset face-to-face π-π interaction. As the linear hydrogen bonding formation was dominant, the intermolecular excimers, which need sufficient overlap between aromatic regions, could not be achieved in the arrangements. Once mechanical stimuli were applied to both crystalline states, linear hydrogen bonds were disturbed and some luminophores formed excimers, leading to the yellow emission. Though a similar mechanism has been already reported,[31,38,65] compound **1** differs from previously reported mechanochromic luminescent compounds forming hydrogen bonds in that its crystals could exhibit the release of small guest molecules.

Conclusions

We demonstrated that 9,10-bis(phenylethynyl)anthracene derivative **1** formed crystals that have ID toluene pillars inside. In the **1Cr•Tol** crystal, the amide groups of **1** formed linear hydrogen bonds, whose bonding mode caused the offset face-to-face arrangements of the luminophores, resulting in the green emission. Compared to the previous study on compound **2**, introducing 4-hexylphenyl groups instead of 4-isopropylphenyl groups prevented compound **1** from forming two-dimensionally hydrogen-bonded molecular sheets. Consequently, both thermal and mechanical stimuli-induced release of the toluene molecule from the crystal were achieved. The former release was accompanied by a transition to another crystalline state **1Cr**, while retaining both the linear hydrogen bonds and green emission. The latter release resulted from a transition to an amorphous state **1Am**, with colour change from green to yellow, which is attributed to excimer formation between the luminophores. Disturbing the linear hydrogen bonds by mechanical stimuli allowed some luminophores to form excimers in the condensed state.

As compound **1** proved, combining mechanochromic luminescence properties with other dynamic functions allows access to various sophisticated photofunctional materials. Therefore, further investigation on luminophores with amide groups and their external stimuli-responsive behaviour is ongoing in our group.

Experimental

General methods

All reagents and solvents were purchased from Tokyo Kasei, FUJIFILM Wako Pure Chemical Corporation, and Kanto Chemical. All reactions were conducted under a nitrogen atmosphere. Flash silica gel column chromatography was performed with a Biotage Isolera Flash system using Biotage Flash Cartridges. ^{1}H NMR spectra were conducted with a JEOL JNM-ECX 400 spectrometer. All chemical shifts obtained from ^{1}H NMR measurements were reported on the δ-scale in ppm relative to the signal of tetramethylsilane (TMS at 0.00), which worked as an internal standard. Proton-decoupled ^{13}C NMR spectra were conducted with the same spectrometer and all chemical shifts (δ) were quoted in ppm using solvents as the internal standard ($CDCl_3$ at 77.16, THF-d_8 at 67.21). Coupling constants (J) in Hz

Please do not adjust margins

and relative intensities were shown. Matrix-assisted laser desorption ionization time-of-flight (MALDI-TOF) mass spectra were conducted on an AB SCIEX TOF/TOF 5800. Elemental analysis was performed with an Exeter Analytical CE440 Elemental Analyzer. Absorption spectra were conducted on a JASCO V-550. Steady-state fluorescence spectra of solutions were recorded with a JASCO FP-6500 and the obtained spectra were corrected for the detector nonlinearity. Time-resolved fluorescence measurements were carried out with a Hamamatsu Photonics Quantaurus-Tau. Photoluminescence quantum efficiencies were measured with a Hamamatsu Photonics Quantaurus-QY. Powder X-ray diffraction measurements were carried out with a Rigaku SmartLab. DSC measurements were conducted using Hitachi DSC7020 with a heating rate of 10 °C min^{-1} under nitrogen atmosphere. TGA was conducted using a Rigaku Thermo plus TG8120 with a heating rate of 10 °C min^{-1} under nitrogen condition. IR measurements were conducted on a JASCO FT/IR-6100 with an ATR unit.

Single crystal X-ray structure analysis

A single crystal of **1Cr•Tol** was mounted on a cryoloop with Paratone®-N (Hampton Research). Crystallographic data was collected using a Rigaku MicroMax-007HF diffractometer and Pilatus 200K detector with Cu Kα radiation (λ = 1.54184 Å) at 173 K. Data collection was conducted with CrystalClear-SM Expert 2.1 (ver. b29).[94] Cell refinement and data reduction were performed with CrysAlis^{PRO}.[95] The initial structure was solved using SHELXT software[96] and expanded using Fourier techniques and refined on F^2 by the full-matrix least-squares method SHELXL-2018/3[97] compiled into Yadokari-XG.[98,99] All parameters were refined using anisotropic temperature factors, except for hydrogen atoms, which were refined using the riding model, with a fixed C–H bond distance. The crystallographic data is summarized in Table S1. CCDC 1999604 (crystal of **1Cr•Tol**) contains the supplementary crystallographic data for this paper. This data is provided free of charge by The Cambridge Crystallographic Data Centre via www.ccdc.cam.ac.uk/data_request/cif.

Conflicts of interest

There are no conflicts to declare.

Acknowledgements

The authors would like to thank Mr. Y. Okado for synthesising the compounds and Ms. A. Tokumitsu, at the Global Facility Center of Hokkaido University, for elemental analysis. The authors also thank Prof. Y. Urano for measuring the photoluminescent quantum yield. This work was supported by JSPS KAKENHI (grant nos. JP18H02024, JP18H01949, and JP19K15517).

Notes and references

1. Y. Sagara, S. Yamane, M. Mitani, C. Weder and T. Kato, *Adv. Mater.*, 2016, **28**, 1073–1095.
2. Y. Sagara and T. Kato, *Nat. Chem.*, 2009, **1**, 605–610.
3. K. Araki and T. Mutai, *Photochemistry*, 2016, **43**, 191–225.
4. T. Kato, J. Uchida, T. Ichikawa and T. Sakamoto, *Angew. Chem. Int. Ed.*, 2018, **57**, 4355–4371.
5. Z. Chi, X. Zhang, B. Xu, X. Zhou, C. Ma, Y. Zhang, S. Liu and J. Xu, *Chem. Soc. Rev.*, 2012, **41**, 3878–3896.
6. X. Zhang, Z. Chi, Y. Zhang, S. Liu and J. Xu, *J. Mater. Chem. C*, 2013, **1**, 3376–3390.
7. Z. Ma, Z. Wang, M. Teng, Z. Xu and X. Jia, *Chemphyschem*, 2015, **16**, 1811–1828.
8. L. Maggini and D. Bonifazi, *Chem. Soc. Rev.*, 2012, **41**, 211–241.
9. A. Seeboth, D. Lotzsch, R. Ruhmann and O. Muehling, *Chem. Rev.*, 2014, **114**, 3037–3068.
10. J. Mei, N. L. C. Leung, R. T. K. Kwok, J. W. Y. Lam and B. Z. Tang, *Chem. Rev.*, 2015, **115**, 11718–11940.
11. R. Davis, N. P. Rath and S. Das, *Chem. Commun.*, 2004, 74–75.
12. T. Mutai, H. Satou and K. Araki, *Nat. Mater.*, 2005, **4**, 685–687.
13. A. Kishimura, T. Yamashita, K. Yamaguchi and T. Aida, *Nat. Mater.*, 2005, **4**, 546–549.
14. T. Mutai, H. Tomoda, T. Ohkawa, Y. Yabe and K. Araki, *Angew. Chem. Int. Ed.*, 2008, **47**, 9522–9524.
15. N. S. S. Kumar, S. Varghese, N. P. Rath and S. Das, *J. Phys. Chem. C*, 2008, **112**, 8429–8437.
16. Y. Zhao, H. Gao, Y. Fan, T. Zhou, Z. Su, Y. Liu and Y. Wang, *Adv. Mater.*, 2009, **21**, 3165–3169.
17. Y. Sagara, M. Karman, E. Verde–Sesto, K. Matsuo, Y. Kim, N. Tamaoki and C. Weder, *J. Am. Chem. Soc.*, 2018, **140**, 1584–1587.
18. Y. Sagara, M. Karman, A. Seki, M. Pannipara, N. Tamaoki and C. Weder, *ACS Cent. Sci.*, 2019, **5**, 874–881.
19. T. Muramatsu, Y. Sagara, H. Traeger, N. Tamaoki and C. Weder, *ACS Appl. Mater. Interfaces*, 2019, **11**, 24571–24576.
20. T. Yamakado, K. Otsubo, A. Osuka and S. Saito, *J. Am. Chem. Soc.*, 2018, **140**, 6245–6248.
21. D. A. Davis, A. Hamilton, J. Yang, L. D. Cremar, D. Van Gough, S. L. Potisek, M. T. Ong, P. V. Braun, T. J. Martinez, S. R. White, J. S. Moore and N. R. Sottos, *Nature*, 2009, **459**, 68–72.
22. C. Löwe and C. Weder, *Adv. Mater.*, 2002, **14**, 1625–1629.
23. B. R. Crenshaw and C. Weder, *Chem. Mater.*, 2003, **15**, 4717–4724.
24. Y. Chen, A. J. H. Spiering, S. Karthikeyan, G. W. M. Peters, E. W. Meijer and R. P. Sijbesma, *Nat. Chem.*, 2012, **4**, 559–562.
25. T. Kosuge, X. Zhu, V. M. Lau, D. Aoki, T. J. Martinez, J. S. Moore and H. Otsuka, *J. Am. Chem. Soc.*, 2019, **141**, 1898–1902.
26. K. Mase, Y. Sasaki, Y. Sagara, N. Tamaoki, C. Weder, N. Yanai and N. Kimizuka, *Angew. Chem. Int. Ed.*, 2018, **57**, 2806–2810.
27. S. Yamane, Y. Sagara and T. Kato, *Chem. Commun.*, 2009, 3597–3599.
28. T. Seki, K. Ida, H. Sato, S. Aono, S. Sakaki and H. Ito, *Chem. Eur. J.*, 2020, **26**, 735–744.
29. T. Seki, T. Ozaki, T. Okura, K. Asakura, A. Sakon, H. Uekusa and H. Ito, *Chem. Sci.*, 2015, **6**, 2187–2195.
30. R. Kaneko, Y. Sagara, S. Katao, N. Tamaoki, C. Weder and H. Nakano, *Chem. Eur. J.*, 2019, **25**, 6162–6169.
31. Y. Sagara, T. Mutai, I. Yoshikawa and K. Araki, *J. Am. Chem. Soc.*, 2007, **129**, 1520–1521.
32. J. Kunzelman, M. Kinami, B. R. Crenshaw, J. D. Protasiewicz and C. Weder, *Adv. Mater.*, 2008, **20**, 119–122.
33. Y. Ooyama, Y. Kagawa, H. Fukuoka, G. Ito and Y. Harima, *Eur. J. Org. Chem.*, 2009, **2009**, 5321–5326.
34. H. Ito, T. Saito, N. Oshima, N. Kitamura, S. Ishizaka, Y. Hinatsu, M. Wakeshima, M. Kato, K. Tsuge and M. Sawamura, *J. Am. Chem. Soc.*, 2008, **130**, 10044–10045.
35. Y. Sagara and T. Kato, *Angew. Chem. Int. Ed.*, 2008, **47**, 5175–5178.

 This journal is © The Royal Society of Chemistry 20xx

Please do not adjust margins

Please do not adjust margins

36. S.-J. Yoon, J. W. Chung, J. Gierschner, K. S. Kim, M.-G. Choi, D. Kim and S. Y. Park, *J. Am. Chem. Soc.*, 2010, **132**, 13675–13683.
37. G. Zhang, J. Lu, M. Sabat and C. L. Fraser, *J. Am. Chem. Soc.*, 2010, **132**, 2160–2162.
38. M. Sase, S. Yamaguchi, Y. Sagara, I. Yoshikawa, T. Mutai and K. Araki, *J. Mater. Chem.*, 2011, **21**, 8347.
39. Y. Sagara and T. Kato, *Angew. Chem. Int. Ed.*, 2011, **50**, 9128–9132.
40. X. Luo, J. Li, C. Li, L. Heng, Y. Q. Dong, Z. Liu, Z. Bo and B. Z. Tang, *Adv. Mater.*, 2011, **23**, 3261–3265.
41. M. S. Kwon, J. Gierschner, S. J. Yoon and S. Y. Park, *Adv. Mater.*, 2012, **24**, 5487–5492.
42. J. Wang, J. Mei, R. Hu, J. Z. Sun, A. Qin and B. Z. Tang, *J. Am. Chem. Soc.*, 2012, **134**, 9956–9966.
43. H. Ito, M. Muromoto, S. Kurenuma, S. Ishizaka, N. Kitamura, H. Sato and T. Seki, *Nat. Commun.*, 2013, **4**, 2009.
44. K. Nagura, S. Saito, H. Yusa, H. Yamawaki, H. Fujihisa, H. Sato, Y. Shimoikeda and S. Yamaguchi, *J. Am. Chem. Soc.*, 2013, **135**, 10322–10325.
45. W. Z. Yuan, Y. Tan, Y. Gong, P. Lu, J. W. Lam, X. Y. Shen, C. Feng, H. H. Sung, Y. Lu, I. D. Williams, J. Z. Sun, Y. Zhang and B. Z. Tang, *Adv. Mater.*, 2013, **25**, 2837–2843.
46. S. Yagai, S. Okamura, Y. Nakano, M. Yamauchi, K. Kishikawa, T. Karatsu, A. Kitamura, A. Ueno, D. Kuzuhara, H. Yamada, T. Seki and H. Ito, *Nat Commun.*, 2014, **5**, 4013.
47. Y. Sagara, T. Komatsu, T. Ueno, K. Hanaoka, T. Kato and T. Nagano, *J. Am. Chem. Soc.*, 2014, **136**, 4273–4280.
48. H. J. Kim, D. R. Whang, J. Gierschner, C. H. Lee and S. Y. Park, *Angew. Chem. Int. Ed.*, 2015, **54**, 4330–4333.
49. Z. Wang, Z. Ma, Y. Wang, Z. Xu, Y. Luo, Y. Wei and X. Jia, *Adv. Mater.*, 2015, **27**, 6469–6474.
50. S. K. Park, I. Cho, J. Gierschner, J. H. Kim, J. H. Kim, J. E. Kwon, O. K. Kwon, D. R. Whang, J.-H. Park, B.-K. An and S. Y. Park, *Angew. Chem. Int. Ed.*, 2016, **55**, 203–207.
51. Y. Sagara, A. Lavrenova, A. Crochet, Y. C. Simon, K. M. Fromm and C. Weder, *Chem. Eur. J.*, 2016, **22**, 4374–4378.
52. Z. Ma, Z. Wang, X. Meng, Z. Ma, Z. Xu, Y. Ma and X. Jia, *Angew. Chem. Int. Ed.*, 2016, **55**, 519–522.
53. Y. Sagara, Y. C. Simon, N. Tamaoki and C. Weder, *Chem. Commun.*, 2016, **52**, 5694–5697.
54. M.-S. Yuan, D.-E. Wang, P. Xue, W. Wang, J.-C. Wang, Q. Tu, Z. Liu, Y. Liu, Y. Zhang and J. Wang, *Chem. Mater.*, 2014, **26**, 2467–2477.
55. T. Seki, Y. Takamatsu and H. Ito, *J. Am. Chem. Soc.*, 2016, **138**, 6252–6260.
56. E. Nagata, S. Takeuchi, T. Nakanishi, Y. Hasegawa, Y. Mawatari and H. Nakano, *ChemPhysChem*, 2015, **16**, 3038–3043.
57. M. Okazaki, Y. Takeda, P. Data, P. Pander, H. Higginbotham, A. P. Monkman and S. Minakata, *Chem. Sci.*, 2017, **8**, 2677–2686.
58. Y. Sagara, K. Kubo, T. Nakamura, N. Tamaoki and C. Weder, *Chem. Mater.*, 2017, **29**, 1273–1278.
59. Y. Sagara, C. Weder and N. Tamaoki, *Chem. Mater.*, 2017, **29**, 6145–6152.
60. M. Jin, T. Seki and H. Ito, *J. Am. Chem. Soc.*, 2017, **139**, 7452–7455.
61. M. Jin, T. Sumitani, H. Sato, T. Seki and H. Ito, *J. Am. Chem. Soc.*, 2018, **140**, 2875–2879.
62. Y. Sagara, N. Tamaoki and G. Fukuhara, *ChemPhotoChem*, 2018, **2**, 959–963.
63. S. Nagai, M. Yamashita, T. Tachikawa, T. Ubukata, M. Asami and S. Ito, *J. Mater. Chem. C*, 2019, **7**, 4988–4998.
64. T. Mutai, T. Sasaki, S. Sakamoto, I. Yoshikawa, H. Houjou and S. Takamizawa, *Nat. Commun.*, 2020, **11**, 1824.
65. Y. Sagara, K. Takahashi, T. Nakamura and N. Tamaoki, *Chem. Asian J.*, 2020, **15**, 478–482.
66. R.-B. Lin, Y. He, P. Li, H. Wang, W. Zhou and B. Chen, *Chem. Soc. Rev.*, 2019, **48**, 1362–1389.
67. S. Das, P. Heasman, T. Ben and S. Qiu, *Chem. Rev.*, 2017, **117**, 1515–1563.
68. F. D. Lewis, J.-S. Yang and C. L. Stern, *J. Am. Chem. Soc.*, 1996, **118**, 12029–12037.
69. F. D. Lewis and J.-S. Yang, *J. Phys. Chem. B*, 1997, **101**, 1775–1781.
70. A. P. H. J. Schenning, P. Jonkheijm, E. Peeters and E. W. Meijer, *J. Am. Chem. Soc.*, 2001, **123**, 409–416.
71. F. Würthner, Z. Chen, F. J. M. Hoeben, P. Osswald, C.-C. You, P. Jonkheijm, J. v. Herrikhuyzen, A. P. H. J. Schenning, P. P. A. M. van der Schoot, E. W. Meijer, E. H. A. Beckers, S. C. J. Meskers and R. A. J. Janssen, *J. Am. Chem. Soc.*, 2004, **126**, 10611–10618.
72. P. Jonkheijm, A. Miura, M. Zdanowska, F. J. Hoeben, S. De Feyter, A. P. Schenning, F. C. De Schryver and E. W. Meijer, *Angew. Chem. Int. Ed.*, 2004, **43**, 74–78.
73. J. van Herrikhuyzen, A. Syamakumari, A. P. H. J. Schenning and E. W. Meijer, *J. Am. Chem. Soc.*, 2004, **126**, 10021–10027.
74. F. J. M. Hoeben, P. Jonkheijm, E. W. Meijer and A. P. H. J. Schenning, *Chem. Rev.*, 2005, **105**, 1491–1546.
75. S. Yagai, *J. Photochem. Photobiol. C*, 2006, **7**, 164–182.
76. S. Yagai, T. Seki, T. Karatsu, A. Kitamura and F. Wurthner, *Angew. Chem. Int. Ed.*, 2008, **47**, 3367–3371.
77. A. Ajayaghosh, V. K. Praveen and C. Vijayakumar, *Chem. Soc. Rev.*, 2008, **37**, 109–122.
78. F. Würthner, C. Bauer, V. Stepanenko and S. Yagai, *Adv. Mater.*, 2008, **20**, 1695–1698.
79. F. Würthner, T. E. Kaiser and C. R. Saha-Möller, *Angew. Chem. Int. Ed.*, 2011, **50**, 3376–3410.
80. S. Yagai, M. Usui, T. Seki, H. Murayama, Y. Kikkawa, S. Uemura, T. Karatsu, A. Kitamura, A. Asano and S. Seki, *J. Am. Chem. Soc.*, 2012, **134**, 7983–7994.
81. S. S. Babu, V. K. Praveen and A. Ajayaghosh, *Chem. Rev.*, 2014, **114**, 1973–2129.
82. S. Yagai, *Bull. Chem. Soc. Jpn.*, 2015, **88**, 28–58.
83. F. Würthner, C. R. Saha-Möller, B. Fimmel, S. Ogi, P. Leowanawat and D. Schmidt, *Chem. Rev.*, 2016, **116**, 962–1052.
84. I. Hisaki, C. Xin, K. Takahashi and T. Nakamura, *Angew. Chem. Int. Ed.*, 2019, **58**, 11160–11170.
85. I. Hisaki, Y. Suzuki, E. Gomez, Q. Ji, N. Tohnai, T. Nakamura and A. Douhal, *J. Am. Chem. Soc.*, 2019, **141**, 2111–2121.
86. Y. Sagara, T. Komatsu, T. Terai, T. Ueno, K. Hanaoka, T. Kato and T. Nagano, *Chem. Eur. J.*, 2014, **20**, 10397–10403.
87. Y. Sagara, T. Komatsu, T. Ueno, K. Hanaoka, T. Kato and T. Nagano, *Adv. Funct. Mater.*, 2013, **23**, 5277–5284.
88. Y. Sagara, S. Yamane, T. Mutai, K. Araki and T. Kato, *Adv. Funct. Mater.*, 2009, **19**, 1869–1875.
89. G. A. Jeffery in *An Introduction to Hydrogen Bonding*, Oxford University Press, New York, 1996, pp. 12.
90. E. R. T. Tiekink and J. Zukerman-Schpector (Eds.) *The Importance of Pi-Interactions in Crystal Engineering: Frontiers in Crystal Engineering*, Wiley-VCH, United Kingdom, 2012, pp. 112.
91. Y. Sagara, K. Takahashi, T. Nakamura and N. Tamaoki, *Mol. Syst. Des. Eng.*, 2020, **5**, 205–211.
92. Y. Sagara, C. Weder and N. Tamaoki, *RSC Adv.*, 2016, **6**, 80408–80414.
93. M. Lübtow, I. Helmers, V. Stepanenko, R. Q. Albuquerque, T. B. Marder and G. Fernández, *Chem. Eur. J.*, 2017, **23**, 6198–6205.
94. Rigaku/MSC. CrystalClear. Rigaku/MSC Inc., The Woodlands, Texas, USA, 2005.
95. Rigaku Oxford Diffraction. CrysAlis PRO. Rigaku Oxford Diffraction, Yarnton, England, 2015.
96. G. M. Sheldrick, *Acta Cryst.*, 2015, **A71**, 3–8.
97. G. M. Sheldrick, *Acta Cryst.*, 2015, **C71**, 3–8.

Please do not adjust margins

Please do not adjust margins

98. Yadokari-XG, Software for Crystal Structure Analyses, K. Wakita, 2001.
99. C. Kabuto, S. Akine, T. Nemoto, E. Kwon, *J. Cryst. Soc. Jpn.*, 2009, **51**, 218–224.

 This journal is © The Royal Society of Chemistry 20xx

Please do not adjust margins